Збірник наукових праць. Галузеве машинобудування, будівництво
Academic journal. Industrial Machine Building, Civil Engineering
http://journals.nupp.edu.ua/znp
https://doi.org/10.26906/znp.2021.57.2580

UDC 624.012

Determination of the compressed zone shape of concrete in reinforced concrete T-section beams under biaxial bending

Usenko Yuliia[1]*, Pavlikov Andriy[2]

[1] National University «Yuri Kondratyuk Poltava Polytechnic» https://orcid.org/0000-0001-8039-182X
[2] National University «Yuri Kondratyuk Poltava Polytechnic» https://orcid.org/0000-0002-5654-5849
*Corresponding author E-mail: yulia0111@gmail.com

The method of the calculation case determining for biaxial bent reinforced concrete T-shaped elements using a complete concrete deformation diagram is presented. Analytical dependences are presented in tabular form, according to which it is possible to determine the neutral line position case in the cross-section of the reinforced concrete element. The given analytical dependences use the concrete relative strains level in the most compressed fiber. It allows the determination of the change of the neutral line position from the beginning of loading till the destruction moment of the reinforced concrete beam element. This approach will allow to determine both the bearing capacity and the serviceability limit state of biaxial bent reinforced concrete T-section beams

Keywords: biaxial bending, compressed zone shapes, the neutral line position, reinforced concrete T-section beam, limit states.

Визначення форми стиснутої зони бетону залізобетонних таврових балок, які зазнають косого згинання

Усенко Ю.О.[1]*, Павліков А.М.[2]

[1] Національний університет «Полтавська політехніка імені Юрія Кондратюка»
[2] Національний університет «Полтавська політехніка імені Юрія Кондратюка»
*Адреса для листування E-mail: yulia0111@gmail.com

Викладено методику визначення випадку розрахунку залізобетонних елементів з тавровим поперечним перерізом на дію косого згинання з використанням повної діаграми деформування бетону. Проаналізовано напружено-деформований стан залізобетонних таврових балок, для опису якого необхідно знати, як у поперечному перерізі розташовується нейтральна лінія, положення якої характеризується такими параметрами: висотою стиснутої зони X, кутом нахилу θ нейтральної лінії до горизонтальної вісі та рівнем відносних деформацій бетону в найбільш стиснутій фібрі η_m. Складність визначення параметрів полягає у різноманітності форм, яких може набувати стиснута зона бетону: трикутник, трапеція, п'ятикутник та шестикутник Представлено три групи форм, кожна з яких містить у собі чотири випадки розташування нейтральної лінії в перерізі. Продемонстровано, як відбувається перехід однієї форми стиснутої зони в іншу при збільшенні кута нахилу зовнішньої силової площини в кожній з трьох груп форм. Вивчено, які граничні випадки можуть виникати при переході від однієї форми до іншої. Зазначено, за якими виразами визначається приналежність до однієї з трьох груп форм. Представлено у табличній формі аналітичні залежності, за якими можна визначити випадок положення нейтральної лінії у перерізі залізобетонного елемента. У наведених аналітичних залежностях використовується рівень відносних деформацій бетону в найбільш стиснутій фібрі поперечного перерізу залізобетонного елемента таврового профілю, що дає змогу визначати зміну положення нейтральної лінії від початку прикладання навантаження до моменту руйнування залізобетонного балкового елемента. Такий підхід дозволить виконувати розрахунки залізобетонних таврових балок, що зазнають косого згинання, як за несучою здатністю, так і за придатністю до нормальної експлуатації

Ключові слова: косе згинання, форма стиснутої зони, положення нейтральної лінії, залізобетонна таврова балка, граничні випадки.

Introduction

For the development of the construction industry, there is a need to constantly improve knowledge about the processes that occur in structures from external loads.

A significant number of the reinforced concrete beam elements in buildings and structures are influenced by causes that bring about complex types of deformation – biaxial bending and torsion. Therefore, there is a need for a more accurate stress-strain state analysis of such elements, for which the priority is to determine the neutral line position in the normal section.

Review of research sources and publications

Studies of beam elements under influence of complex deformations are clarified in [1 – 9]. The analysis of the stress-strain state in the biaxial bent beam elements with the rectangular section is presented in [5 – 7], and with the T-section – in [1, 5].

Definition of unsolved aspects of the problem

The description of the compressed zone forming process in the T-section reinforced concrete elements is presented using rectangular [1] and two-line [5] stress distribution diagrams in the compressed concrete zone of the normal cross-section. Differentiation of calculation cases for T-section elements using a complete diagram of concrete deformation was not observed.

Problem statement

In calculations of both the bearing capacity and the serviceability limit state to describe the stress-strain state of a biaxial bent T-section reinforced concrete beam, it is necessary to know how the neutral line is located in its cross-section under the influence of external load. Therefore, the aim is to show how the forms of the compressed concrete zone are systematized into groups and how the calculation case for the T-section elements is determined.

Basic material and results

According to the analysis of literature sources, in reinforced concrete T-section beams under the influence of external load, the phenomenon of biaxial bending almost always occurs.

External load causes changes in the stress-strain state of the beam element. In order to describe this state, it is necessary to know how the neutral line (the line that separates the compressed and stretched zones of concrete) is located in the cross-section. Its position in turn is characterized by the following parameters: the height X of the concrete compressed zone, the angle θ of neutral line inclination to the horizontal axis, and the value of the concrete relative strain level in the most compressed fiber η_m. The analysis has shown that the values of these parameters can generally vary within the following limits: $0 \le \theta \le 90^o$, $0 \le X \le h\cos\theta$, $0 \le \eta_m \le 2{,}7$. They can be used as boundary characteristics.

All possible causes of the neutral line position in the normal section of the reinforced concrete T-section beam are systematized into three groups (Tables 1 – 3). Analytical dependencies are used to determine belonging to one of the three groups:

$$0 < X \le 0{,}5h_{eff}, \tag{1}$$

$$0{,}5 < X \le 0{,}5h_{eff}\left(1+\frac{b_{eff,1}}{b_{eff}}\right), \tag{2}$$

$$0{,}5h_{eff}\left(1+\frac{b_{eff,1}}{b_{eff}}\right) < X \le h_{eff}, \tag{3}$$

where b_{eff}, $h_{eff.}$ $b_{eff,1}$ – geometric parameters of the T-shaped cross-section in the reinforced concrete bending element;

X – the height of the compressed concrete zone under simple bending, which is determined using the formula

$$X = \frac{f_{yd}A_s}{f_{cd}b_{eff}\omega(\theta;\eta_m)}, \tag{4}$$

where f_{yd} – the calculated value of the tensile reinforcement resistance;

f_{cd} – the calculated value of the concrete compressive strength;

A_s – the cross-sectional area of the reinforcement;

ω (θ; η_m) – the completeness coefficient of the stress distribution diagram in the compressed concrete zone under simple bending.

With increasing the angle of the external force plane inclination in each group, there is a change from one form to another in a certain sequence. When transferring from one form to another, the neutral line occupies a certain limit position, which reduces the number of unknown geometric parameters. This makes it possible to determine at what angle the inner force plane is inclined with such a neutral line position. Using the parallel criterion for planes of external and internal moments action, the conventional angle β' can be determined with the formula

$$\beta' = arctg\left(\frac{d_b - x_{0,Nc}}{d_h - y_{0,Nc}}\right), \tag{5}$$

where d_b, d_h – the projections of the distance from the most compressed concrete fiber to the application point of stress resultant in stretched reinforcement on the X_0 та Y_0 axes respectively.

Tables 1 – 3 show the analytical dependences that allow to calculate the value of the inclination angle of the force plane for each limit case in each group. The derivation of the completeness coefficients of the stress distribution diagram in the compressed concrete zone under complex bending is described in [10].

To determine the case of the neutral line position in the group, it is necessary to compare the actual inclination angle of the external force plane to the vertical axis with the conditional angle of the internal force plane for extreme cases. If the actual inclination angle is greater than the conditional angle of the first limit case in one of the three groups, it is necessary to proceed to the comparison with the conditional angle of the second limit case. If it is greater again, then compare with the third limit case, and if smaller, the compression zone actual shape is between the first and second limit cases.

Table 1 – The first group of shapes

Shapes of the compressed zone	Limit cases
1.1 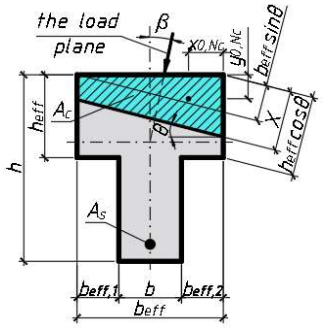 $b_{eff}\sin\theta < X < h_{eff}\cos\theta$	$A_c = \frac{f_{yd}\ A_s}{f_{cd}};\quad \omega_1 = \frac{\eta_m(4-\eta_m)}{6};\quad \omega_2 = 1-(1-\gamma_2)^3\left(1+\frac{\eta_m\gamma_2}{(4-\eta_m)}\right);$ $\varphi_{x1} = \varphi_{y1} = \frac{\eta_m\ (5-\eta_m)}{30};\quad \varphi_{x2} = 1-(1-\gamma_2)^3\left(1+3\gamma_2+\frac{4\eta_m\gamma_2^2}{5-\eta_m}\right);$ $\varphi_{y2} = 1-(1-\gamma_2)^4\left(1+\frac{\eta_m\gamma_2}{5-\eta_m}\right)$
1.2 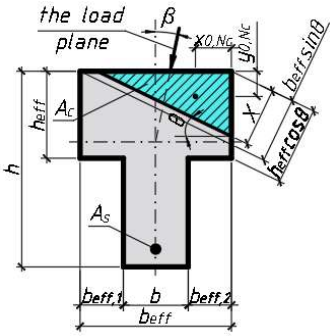 $b_{eff}\sin\theta > X < h_{eff}\cos\theta$	1.1 – 1.2 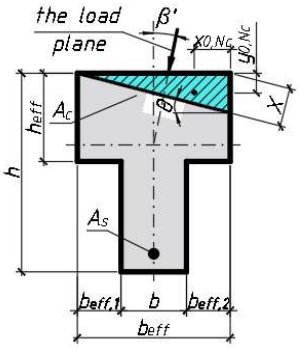 $x_{0,Nc} = \frac{b_{eff}\,\varphi_{y1}}{\omega_1}$ $y_{0,Nc} = \frac{b_{eff}\,tg\theta\varphi_{x1}}{\omega_1}$
1.3 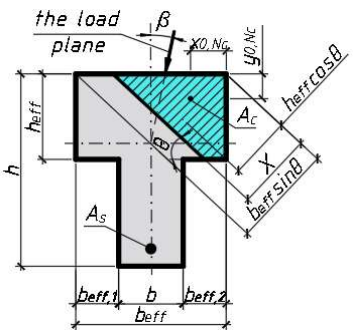 $h_{eff}\cos\theta < X < b_{eff}\sin\theta$	1.2 – 1.3 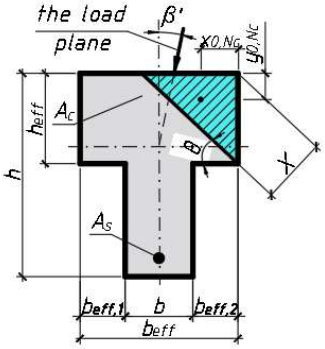 $x_{0,Nc} = \frac{h_{eff}\,\varphi_{y1}}{tg\theta\omega_1}$ $y_{0,Nc} = \frac{h_{eff}\,\varphi_{x1}}{\omega_1}$
1.4 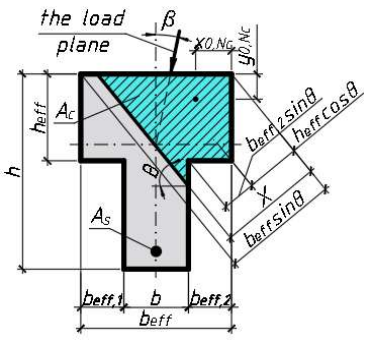 $b_{eff,2}\sin\theta + h_{eff}\cos\theta < X < b_{eff}\sin\theta$	1.3 – 1.4 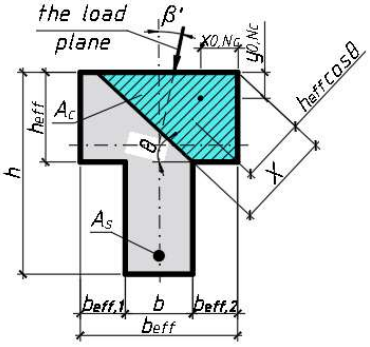 $x_{0,Nc} = \left(\frac{h_{eff}}{tg\theta} + b_{eff,2}\right)\cdot\frac{\varphi_{y1}\varphi_{y2}}{\omega_1\omega_2}$ $y_{0,Nc} = \left(h_{eff} + b_{eff,2}tg\theta\right)\cdot\frac{\varphi_{x1}\varphi_{x2}}{\omega_1\omega_2}$ $\gamma_2 = \frac{h_{eff}}{h_{eff} + b_{eff,2}tg\theta}$

Table 2 – The second group of shapes

Shapes of the compressed zone	Limit cases
2.1 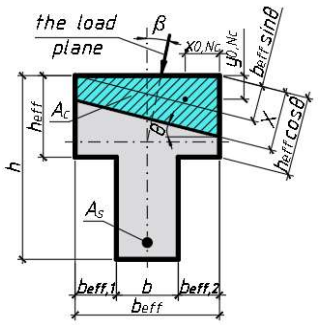 	$A_c = \frac{f_{yd}\ A_s}{f_{cd}}$; $\omega_1 = \frac{\eta_m(4-\eta_m)}{6}$; $\omega_2 = 1-(1-\gamma_2)^3\left(1+\frac{\eta_m\gamma_2}{(4-\eta_m)}\right)$; $\varphi_{x1} = \varphi_{y1} = \frac{\eta_m\ (5-\eta_m)}{30}$; $\varphi_{x2} = 1-(1-\gamma_2)^3\left(1+3\gamma_2+\frac{4\eta_m\gamma_2^2}{5-\eta_m}\right)$; $\varphi_{y2} = 1-(1-\gamma_2)^4\left(1+\frac{\eta_m\gamma_2}{5-\eta_m}\right)$; $\varphi_{x3} = 1-(1-\gamma_1)^4\left(1+\frac{\eta_m\gamma_1}{5-\eta_m}\right)$; $\varphi_{y3} = 1-(1-\gamma_1)^3\left(1+3\gamma_1+\frac{4\eta_m\gamma_1^2}{5-\eta_m}\right)$
$b_{eff}\ sin\theta < X < h_{eff}\ cos\theta$	2.1 – 2.2
2.2 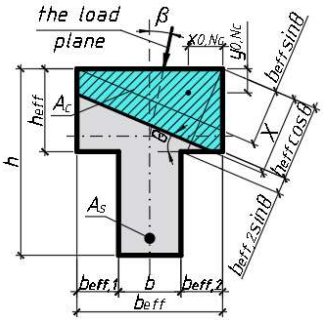 	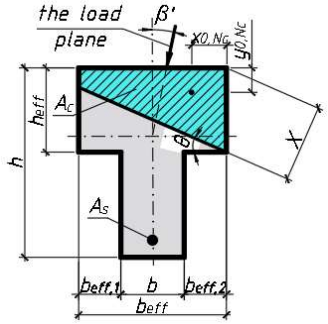 $x_{0,Nc} = \frac{h_{eff}\varphi_{y1}\varphi_{y3}}{tg\theta\omega_1\omega_3}$ $y_{0,Nc} = \frac{h_{eff}\varphi_{x1}\varphi_{x3}}{\omega_1\omega_3}$ $\gamma_1 = \frac{b_{eff}tg\theta}{h_{eff}}$
$b_{eff}\ sin\theta < X < b_{eff,2}\ sin\theta + h_{eff}\ cos\theta$	2.2 – 2.3
2.3 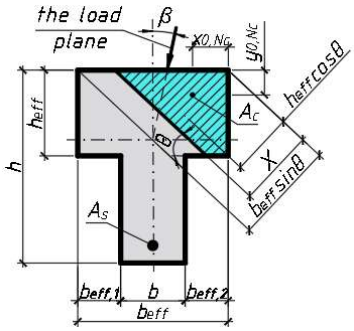 	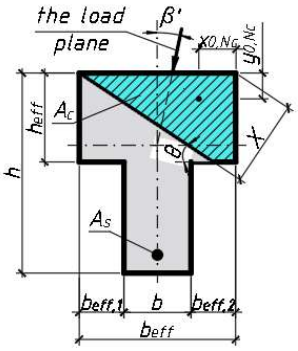 $x_{0,Nc} = \frac{b_{eff}\varphi_{y1}\varphi_{y2}}{\omega_1\omega_2}$ $y_{0,Nc} = \frac{b_{eff}\ tg\theta\varphi_{x1}\varphi_{x2}}{\omega_1\omega_2}$ $\gamma_2 = \frac{h_{eff}}{b_{eff}\ tg\theta}$
$h_{eff}\ cos\theta < X < b_{eff}\ sin\theta$	2.3 –2.4
2.4 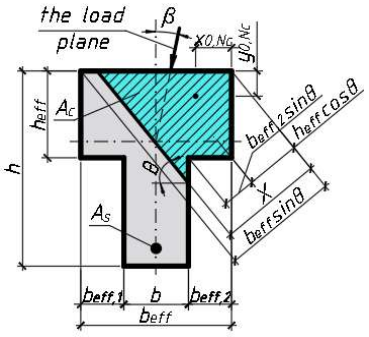 	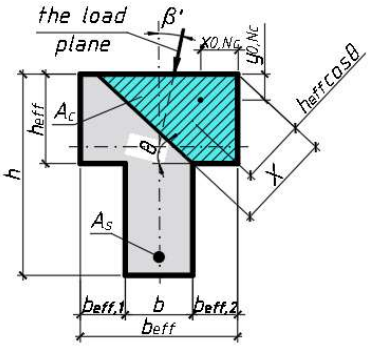 $x_{0,Nc} = \left(\frac{h_{eff}}{tg\theta} + b_{eff,2}\right)\cdot\frac{\varphi_{y1}\varphi_{y2}}{\omega_1\omega_2}$ $y_{0,Nc} = \left(h_{eff} + b_{eff,2}tg\theta\right)\cdot\frac{\varphi_{x1}\varphi_{x2}}{\omega_1\omega_2}$ $\gamma_2 = \frac{h_{eff}}{h_{eff} + b_{eff,2}tg\theta}$
$b_{eff,2}\ sin\theta + h_{eff}\ cos\theta < X < b_{eff}\ sin\theta$	

Table 3 – The third group of shapes

Shapes of the compressed zone	Limit cases
3.1 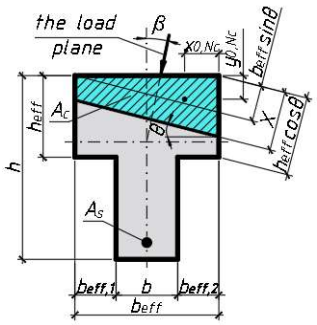	$A_c = \frac{f_{yd}\ A_s}{f_{cd}}$; $\omega_1 = \frac{\eta_m(4-\eta_m)}{6}$; $\omega_2 = 1-(1-\gamma_2)^3\left(1+\frac{\eta_m\gamma_2}{(4-\eta_m)}\right)$; $\varphi_{x1} = \varphi_{y1} = \frac{\eta_m\ (5-\eta_m)}{30}$; $\varphi_{x2} = 1-(1-\gamma_2)^3\left(1+3\gamma_2+\frac{4\eta_m\gamma_2^2}{5-\eta_m}\right)$; $\varphi_{y2} = 1-(1-\gamma_2)^4\left(1+\frac{\eta_m\gamma_2}{5-\eta_m}\right)$; $\varphi_{x3} = 1-(1-\gamma_1)^4\left(1+\frac{\eta_m\gamma_1}{5-\eta_m}\right)$; $\varphi_{y3} = 1-(1-\gamma_1)^3\left(1+3\gamma_1+\frac{4\eta_m\gamma_1^2}{5-\eta_m}\right)$
	3.1 – 3.2
$b_{eff}\ sin\theta < X < h_{eff}\ cos\theta$	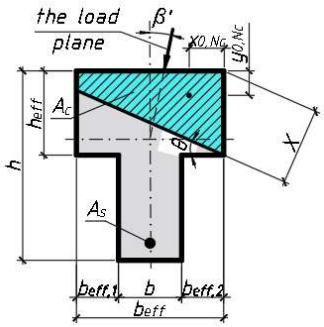 $x_{0,Nc} = \frac{h_{eff}\varphi_{y1}\varphi_{y3}}{tg\theta\omega_1\omega_3}$; $y_{0,Nc} = \frac{h_{eff}\varphi_{x1}\varphi_{x3}}{\omega_1\omega_3}$; $\gamma_1 = \frac{b_{eff}tg\theta}{h_{eff}}$
3.2 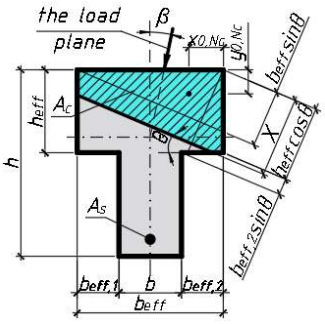	3.2 – 3.3
$b_{eff}\ sin\theta < X < b_{eff,2}\ sin\theta + h_{eff}\ cos\theta$	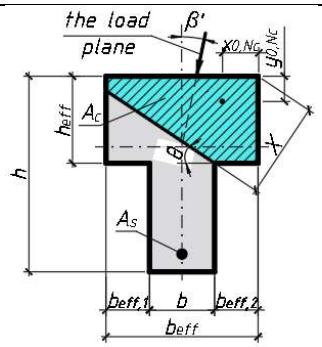 $x_{0,Nc} = \left(\frac{h_{eff}}{tg\theta} + b_{eff,2}\right) \times \frac{\varphi_{y1}\left(\varphi_{y2}-\varphi_{y3}-1\right)}{\omega_1(\omega_2+\omega_3-1)}$; $y_{0,Nc} = \left(h_{eff} + b_{eff,2}tg\theta\right) \times \frac{\varphi_{x1}\left(\varphi_{x3}-\varphi_{x2}-1\right)}{\omega_1(\omega_2+\omega_3-1)}$
3.3 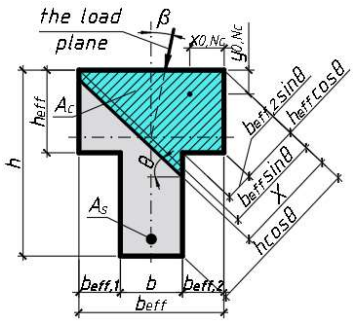	$\gamma_1 = \frac{b_{eff}tg\theta}{h_{eff} + b_{eff,2}tg\theta}$; $\gamma_2 = \frac{h_{eff}}{h_{eff} + b_{eff,2}tg\theta}$
	3.3 –3.4
$h_{eff}\ cos\theta < X < b_{eff}\ sin\theta$	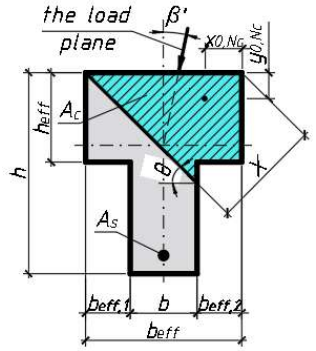 $x_{0,Nc} = \frac{b_{eff}\varphi_{y4}}{\omega_1\cdot(\omega_2+\omega_4)}$; $y_{0,Nc} = \frac{b_{eff}tg\theta\varphi_{x4}}{\omega_1\cdot(\omega_2+\omega_4)}$; $\gamma_2 = \frac{h_{eff}}{b_{eff}tg\theta}$; $\gamma_3 = \frac{b_{eff,2}}{b_{eff}}$
3.4 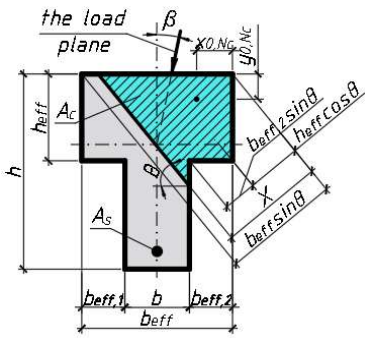	
$b_{eff,2}\ sin\theta + h_{eff}\ cos\theta < X < b_{eff}\ sin\theta$	

Conclusions

Special attention should be paid to T-beams due to the variety of shapes that can be generated in a compressed area of concrete. For convenience, all forms of the compressed concrete zone are systematized into three groups depending on the initial position of the neutral line in the cross-section. In each group, there are limit cases that allow determining the shape of the compressed zone for the biaxial bended reinforced concrete T-beam.

Analytical dependences for determining the inclination angle of the force plane for limit cases are written depending on the level of relative deformations in the compressed zone of concrete, which allows determining how the neutral line is located at different load levels.

The presented method for determining the case of the neutral line position allows determining both the bearing capacity and the serviceability limit state of biaxial bended reinforced concrete T-section beams.

References

1. Хохлов О.Г. (2000). *Влияние точности монтажа крановых рельсов на несущую способность подкрановых железобетонных балок*. (Дис. канд. тех. наук). ПолтНТУ, Полтава

2. Sfakianakis M. (2002). Biaxial bending with axial force of reinforced, composite and repaired concrete sections of arbitrary shape by fiber model and computer graphics. *Advances in Engineering Software*, 33(4), 227-242 https://doi.org/10.1016/S0965-9978(02)00002-9

3. Bonet J.L., Romero M.L., Miguel P.F., Fernandez M.A. (2004). A fast stress integration algorithm for reinforced concrete sections with axial loads and biaxial bending. *Computers&Structures,* 82(2–3), 213-225 https://doi.org/10.1016/j.compstruc.2003.10.009

4. Bonet J.L., Barros M.H.F.M., Romero M.L. (2006). Comparative study of analytical and numerical algorithms for designing reinforced concrete sections under biaxial bending. *Computers&Structures*, 84(31-32), 2184-2193 https://doi.org/10.1016/j.compstruc.2006.08.065

5. Дяченко Є.В. (2006). *Розрахунок міцності косозігнутих залізобетонних елементів з урахуванням повної діаграми фізичного стану бетону*. (Дис. кан. тех. наук). ПолтНТУ, Полтава

6. Павліков А.М. (2007). *Напружено-деформований стан навскісно завантажених залізобетонних елементів у закритичній стадії*. (Дис. док. тех. наук). ПолтНТУ, Полтава

7. Бойко О.В. (2009). *Оцінка міцності навскісно зігнутих балок на основі дволінійних розрахункових діаграм деформування бетону та арматури*. (Дис. кан. тех. наук). ПолтНТУ, Полтава

8. Харченко М.О. (2013). *Розрахунок міцності косозігнутих залізобетонних балок таврового профілю з урахуванням нелінійного деформування бетону та арматури* (Дис. кан. тех. наук). ПолтНТУ, Полтава

9. Vaz Rodrigues R. (2015). A new technique for ultimate limit state design of arbitrary shape RC sections under biaxial bending. *Engineering Structures*, 104, 1-17 https://doi.org/10.1016/j.engstruct.2015.09.016

10. Prykhodko Yu., Pavlikov A. (2020). *The change of stress-strain state in biaxial bended reinforced concrete T-section beams depending on the load*. 13th edition of the fib International PhD Symposium in Civil Engineering, France, 230-236

1. Khokhlov O.G. (2000). *Influence of crane rails installation on the bearing capacity of crane reinforced concrete beams*. (Diss. for the degree of PhD). PoltNTU, Poltava

2. Sfakianakis M. (2002). Biaxial bending with axial force of reinforced, composite and repaired concrete sections of arbitrary shape by fiber model and computer graphics. *Advances in Engineering Software*, 33(4), 227-242 https://doi.org/10.1016/S0965-9978(02)00002-9

3. Bonet J.L., Romero M.L., Miguel P.F., Fernandez M.A. (2004). A fast stress integration algorithm for reinforced concrete sections with axial loads and biaxial bending. *Computers&Structures,* 82(2–3), 213-225 https://doi.org/10.1016/j.compstruc.2003.10.009

4. Bonet J.L., Barros M.H.F.M., Romero M.L. (2006). Comparative study of analytical and numerical algorithms for designing reinforced concrete sections under biaxial bending. *Computers&Structures*, 84(31-32), 2184-2193 https://doi.org/10.1016/j.compstruc.2006.08.065

5. Dyachenko E.V. (2006). *Strength calculation of biaxial bended reinforced concrete elements using the full diagram of the concrete physical state*. (Diss. for the degree of PhD). PoltNTU, Poltava

6. Pavlikov A.M. (2007). *Stress-strain state of biaxial loaded reinforced concrete elements in the supercritical stage*. (Diss. for the degree of DSc). PoltNTU, Poltava

7. Boyko O.V. (2009). *Estimation of biaxial bended beams strength using two-line concrete and steel reinforcing deformation diagrams*. (Diss. for the degree of PhD). PoltNTU, Poltava

8. Kharchenko M.O. (2013). *Calculation of biaxial bended reinforced concrete T-beams strength using nonlinear concrete and reinforcement deformation*. (Diss. for the degree of PhD). PoltNTU, Poltava

9. Vaz Rodrigues R. (2015). A new technique for ultimate limit state design of arbitrary shape RC sections under biaxial bending. *Engineering Structures*, 104, 1-17 https://doi.org/10.1016/j.engstruct.2015.09.016

10. Prykhodko Yu., Pavlikov A. (2020). *The change of stress-strain state in biaxial bended reinforced concrete T-section beams depending on the load*. 13th edition of the fib International PhD Symposium in Civil Engineering, France, 230-236